Thermal Analysis Technique Applied to a Conformal Phased Array Antenna

Kevin Campion,* Joseph J. Gallagher,† Leo R. Paradis,‡ and Francis A. Shukis §
Raytheon Company, Bedford, Massachusetts

Development of an advanced interceptor vehicle instrumentation system required the thermal analysis of a conformal phased array antenna subjected to hypersonic flight velocities. Thermal, structural, and electrical considerations mandated that three-dimensional temperature fields in a charring, ablating medium be developed. The approach taken to solve the problem was to develop boundary conditions via multiple one-dimensional charring ablation analyses and impose these on a three-dimensional temperature analysis model, using a graphics-oriented preprocessing routine. A time-temperature boundary condition was imposed on the three-dimensional model at a depth below the preflight external surface. The in-depth temperature fields that were developed were then used with a structural analysis routine to estimate material stress levels during flight. The computer codes used in this analysis were all well established in their respective areas of application.

Introduction

ADVANCED interceptor missiles will be required to perform in an active radio-frequency (RF) mode during the stresses of high-speed atmospheric entry and flight. Traditional structural protective techniques such as insulating material layers thus assume the added burden of providing high-quality RF windows.

A photograph of a mock-up of the flight vehicle is shown in Fig. 1. The vehicle is a high-aspect-ratio cone, and the RF antenna array is located well aft of the tip. Figure 2 presents a cross-section pictorial of the vehicle with some of the equipment required for a passive flight experiment. Of particular interest is the array of RF windows, which penetrates the heat shield, shown in plan view in Fig. 3.

The RF window array occupies a location on the nominally lee side of the vehicle, encompassing an arc of about 20 deg. The array and its surrounding material are inserted into the flight vehicle thermal protection system, as shown in the pictorial view. Window material is slip-cast fused silica similar to that often used in guided missile radome applications. Encompassing the windows is an insert of graphite-loaded, tape-wound carbon phenolic with a 20-deg wrap angle. Adjacent to the array insert is a thinner section of silica phenolic, which forms the heat shield for the remainder of the vehicle. Electrical components are located at the base of the windows, along with structural support members as shown in Fig. 2.

Operationally, vehicle launch from ground level is followed by an exoatmospheric ballistic flight phase, during which the entry vehicle is protected by a shroud. After shroud jettison and entry, the vehicle flies a pullup and cruise trajectory, followed by a terminal dive. Severe heating is experienced during a large portion of the latter stages of the flight, with peak heating occurring during pull-up. A flight control computer is programmed to ensure that the array insert is leeward during pull-up. After the vehicle flight path has leveled, a number of roll angles and angles of attack (Fig. 4) are flown to satisfy mission requirements.

The problem posed to thermal/structural analysts was to determine the impact of the proposed flight path on the insert, in terms of: 1) surface recession rates, 2) magnitude and location of thermal stresses in the insert assembly, and 3) temperature levels in the supporting structure and its impact on electrical components.

The problem solution consisted of developing a three-dimensional model of a repetitive array section across the span from the windows to the silica phenolic. Temperature boundary conditions were applied at the model surface, these having been developed from one-dimensional analyses. Model surface was taken at a depth of 0.25 in. (6.4 mm) from the preflight external surface, a value selected from inspection of the same one-dimensional analyses. This process developed temperature data throughout the insert for the purpose of component operating temperature and thermal stress evaluations.

Analytical Approach

In the development of an analytical approach, numerous factors were considered and resolved. It was known a priori that development of a multidimensional model that encompassed the entire aerodynamic effect from surface recession and charring to structural temperature predictions was financially impractical. Therefore, it was decided to utilize one-dimensional charring material ablation analyses to develop boundary conditions for a more complex multidimensional model, the boundary conditions to be imposed at a predetermined depth in the larger model where no recession was predicted. This approach has been used successfully in prior projects, achieving good comparisons between in-depth temperature predictions and flight test data.

A further consideration in evaluating the complexity of the required analyses is the use of variable thermodynamic transport properties as opposed to constant average values. Estimates of computational time utilizing both approaches revealed almost an order-of-magnitude increase when variable properties were used in multidimensional analyses. An alternative, lower-cost approach was developed, where average

Presented as Paper 84-1762 at the AIAA 19th Thermophysics Conference, Snowmass, CO, June 25-28, 1984; received Feb. 25, 1985; revision received Oct. 19, 1985.

*Engineer, Engineering Analysis and Test Department, Missile Systems Division. Member AIAA.

†Staff Engineer, Engineering Analysis and Test Department, Missile Systems Division. Member AIAA.

‡Principal Engineer, Engineering Analysis and Test Department, Missile Systems Division. Member AIAA.

§Senior Engineer, Engineering Analysis and Test Department, Missile Systems Division. Member AIAA.

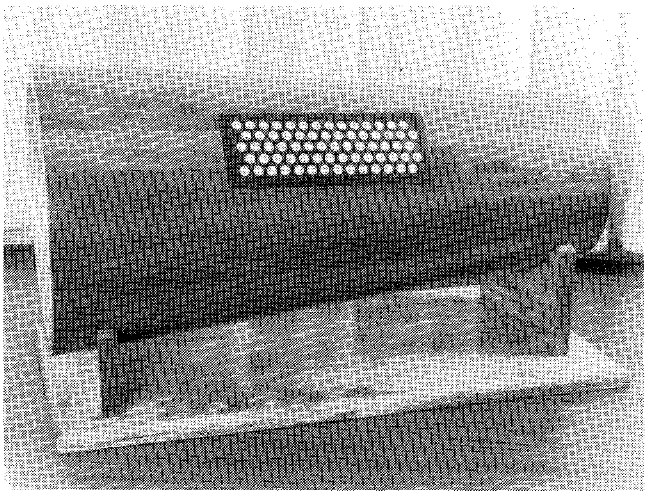

Fig. 1 Mock-up of flight vehicle.

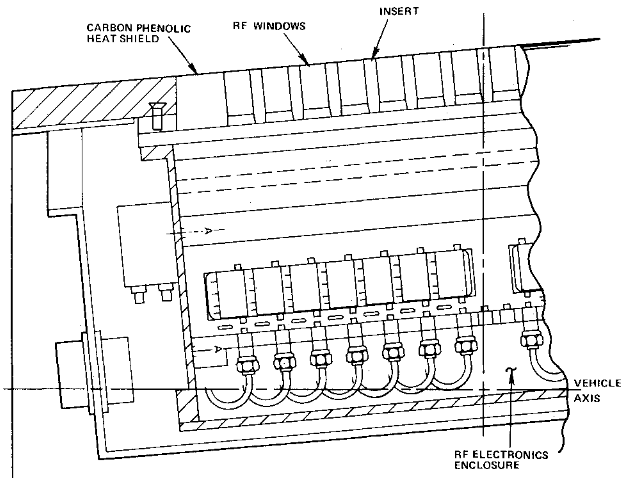

Fig. 2 Cross-section pictorial of vehicle.

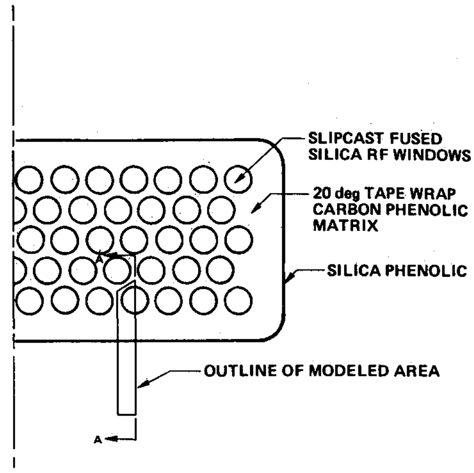

Fig. 3 Insert with outline of area modeled in three-dimensional finite element model.

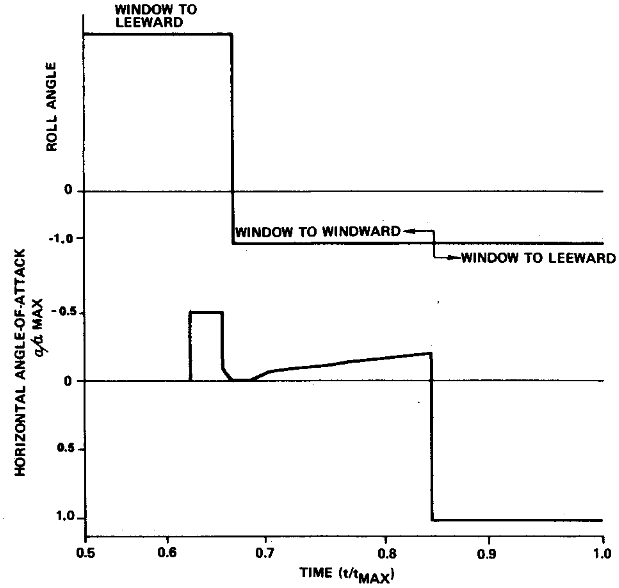

Fig. 4 Angle-of-attack history.

thermal properties were developed by examination of supplemental one-dimensional analyses, and these were imposed on the multidimensional analysis.

The material deleted from the model by imposition of the temperature boundary condition was included later to reform a complete thickness (minus surface erosion) structure in the structural analysis model. Temperatures for this material were those developed by the one-dimensional analyses. The basic assumption here was that, in an area of extensive surface erosion and charring, the heat flow over a small dimension would be governed by one-dimensional surface effects as opposed to multidimensional structural effects.

Another group of considerations involved the geometrical extent and matrix size of the multidimensional analysis. Since the circular/triangular window geometry did not lend itself to a two-dimensional analysis, it was decided to construct a three-dimensional model to obtain the desired refinement of thermal data.

Preliminary conservative studies on stresses in the window assembly due to thermal loading indicated that the highest stresses were occurring in the carbon phenolic at a location adjacent to the stainless steel doubler. Because the stresses in the carbon phenolic are highly dependent on temperature gradient as well as total temperature rise, it was decided to use a large quantity of elements in the thermal analysis to develop the required accuracy.

A study flow diagram is shown in Fig. 5. A critical component in the performance of the study was the use of compatible analysis and element generation routines: ADINAT[1] (Automatic Dynamic Incremental Nonlinear Analysis of Temperature) and GIFTS[2] (Graphics-oriented Interactive Finite Element Time Sharing), along with SAAS-III[3] (see Appendix), all of which had demonstrated their compatibility and usefulness for such a purpose in the past.

Analyses

One-Dimensional Thermal Analyses

Transient temperature boundary conditions for the three-dimensional ADINAT model were generated at four locations, as shown in Fig. 6. Unidimensional temperature profiles were generated at 1) the slip-cast fused silica window, 2) the carbon phenolic insert, 3) the carbon phenolic at insert joint, and 4) the silica phenolic heat shield. A typical profile is shown in Fig. 7; depth is measured from the original surface.

Surface temperatures peaked at 2220 F, 2270 F, and 2510 F for slip-cast fused silica, carbon phenolic, and silica phenolic, respectively. Fluctuations in surface temperatures are in direct response to the roll and angle-of-attack history. At ¼-in. depths, the temperatures at the 4 one-dimensional locations reached maximums of 1095, 1115-1085, and 935°F. These are the temperature histories imposed as boundary conditions for

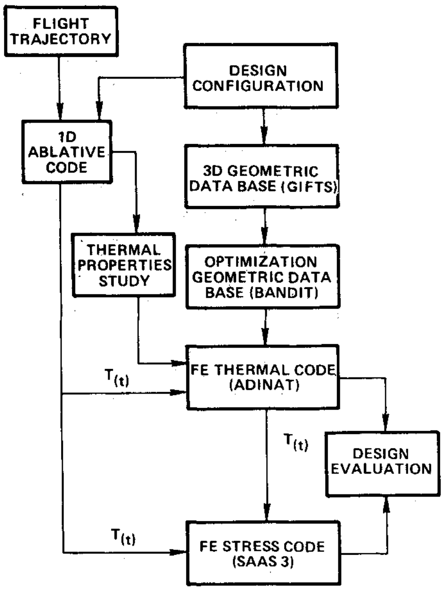

Fig. 5 Analysis flow chart.

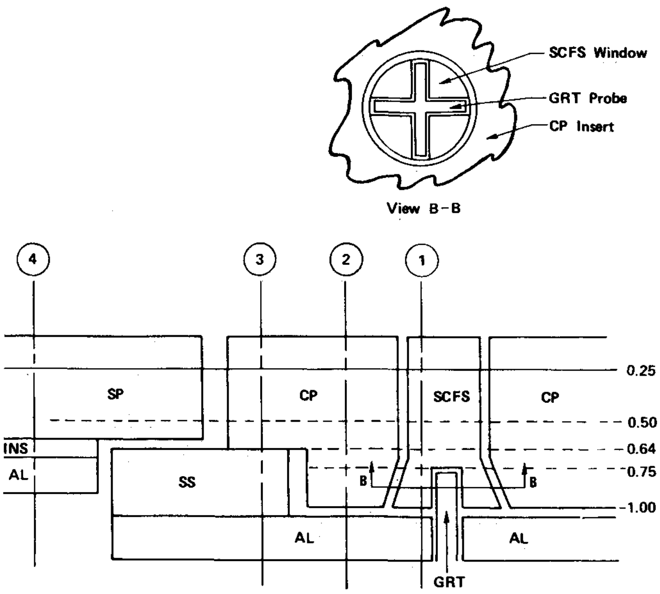

Fig. 6 One-dimensional profile locations (view A-A).

the three-dimensional model, which begins sufficiently below the char depths, as will be shown next.

A modified version[4] of the Charring Material Ablation (CMA) code[5] (see Appendix) was used for the one-dimensional models. Using the automatic node generation scheme of the modified code, the first nodal thickness was .001 in. followed by increasing spacing in the remainder of the ablator and in the backup materials. The variable spacing is referenced to the moving surface (as the front surface recedes, nodes are deleted from the rear). The ablating surface boundary condition was convective heating with coupled mass transfer, including the effects of unequal heat and mass transfer coefficients (nonunity Lewis number). Convective boundary condition data input to CMA were generated by cold-wall aerodynamic heating computations. These data consisted of histories of the recovery enthalpies, edge velocities, edge pressures, and local cold-wall heat-transfer coefficients. Computation of the surface energy balances used data input for each ablator material in the form of surface temperature as a function of mass loss rate, along with enthalpy and chemical-composition data. Chemical properties: reaction rate coefficients, and initial (virgin) and final (charred) densities of carbon phenolic and silica phenolic had been correlated from experimental data.[6]

Ablation predictions for carbon phenolic are shown in Fig. 8. Recession, char, and pyrolysis depths are 0.045, 0.097, and 0.483 in. for carbon phenolic and 0, 0.090 and 0.474 in. for silica phenolic. No slip-cast fused silica mass loss was predicted.

Three-Dimensional Thermal Analysis

The thermal analysis of the insert was governed by the assembly configuration as previously described, as well as by the geometry of an individual silica window. The window is configured so that a cruciform-shaped, glass-reinforced teflon (GRT) RF probe protrudes into its base. A cross-sectional view of the probe/window configuration is shown as section A-A in Fig.3.

The geometry for the finite element model of the insert was created using the GIFTS "model generation" computer code. The scope of this computer codes use was coordinate generation, material property-type designation, degree-of-freedom imposition, and nodal connectivities.

During the modeling of the window assembly, the probe/window interface region was simplified to reduce the complexity of the geometry. This also reduced the cost of the computer runs. The simplifications were made on an equivalent volume basis; i.e., a cylinder of equivalent volume replaced a probe of considerably more complex geometry. The model of the window assembly turned out to be composed of 522 twenty-node

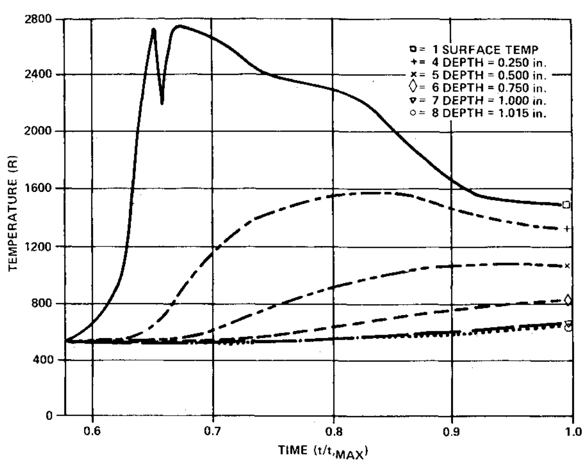

Fig. 7 Carbon phenolic temperature histories (one-dimensional).

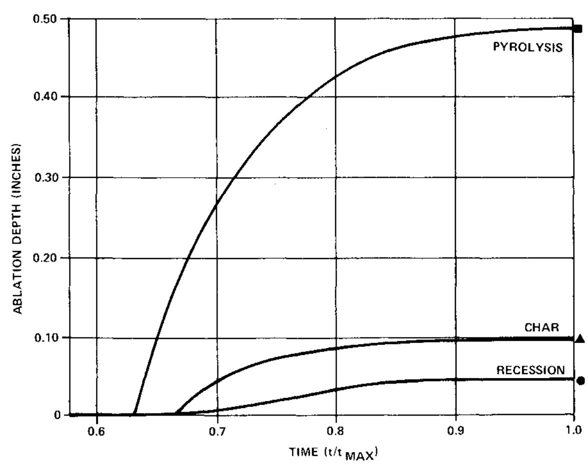

Fig. 8 Carbon phenolic ablation histories.

elements, with a total of 2196 nodes. Drawings of the insert are shown in Figs. 2 and 3. The resulting finite element model is shown in Fig. 9.

The GIFTS-generated data base was then sent through a matrix resequencing routine. The Gibbs, Poole, Stockmeyer[7] method was the strategy used in the resequencing of the three-dimensional finite element model. The results of the matrix resequencing yielded a matrix with a maximum bandwidth of 368 nodes. The geometric data base was then converted by a postprocessing code (internal to GIFTS) to a format compatible with the ADINAT Thermal Analysis code.

Model boundary conditions were as follows: adiabatic boundaries at all model extremities except the top surface of the model. The adiabatic boundary condition was imposed on the three cross-sectional model surfaces that separate the modeled silica element from the other antenna elements. These boundaries were chosen because of anticipated areas of little or no heat transfer owing to geometric symmetry of the RF antenna (see Fig. 3). The adiabatic boundary condition was imposed on the outermost silica phenolic cross-section surface because it was felt that the amount of silica phenolic included in the three-dimensional model of the window was sufficient to simulate any effects on the RF window assembly due to contact with the silica phenolic of the reentry vehicle.

The adiabatic boundary condition on the bottom surface of the model was imposed because the one-dimensional temperature profiles through the carbon phenolic indicated a maximum temperature rise at the aluminum structure of only 100°F. This, coupled with the fact that there would be very low air pressure in contact with the majority of the bottom aluminum surface, justified the adiabatic condition.

The boundary conditions on the top surface were defined by the temperature histories obtained from the one-dimensional thermal analysis conducted on the four prominent material cross sections. The location of temperatures in the one-dimensional analysis that were imposed upon the three-dimensional model were chosen at a depth such that the carbon phenolic was approximately 50% pyrolized (see Fig. 9) at the end of the flight. Thermal property changes from this pyrolization level to the virgin, cooler material at the structure were compensated for by use of equivalent constant values such as would occur at 500°F. Since the carbon phenolic represented the greatest property change among the four different material cross-sectional profiles, it was the material that determined the depth of the top layer of the three-dimensional thermal model. The location of the top layer of the three-dimensional model was reduced by ¼-in. from the original surfaces as a result of this logic process. Thus, the temperature histories at a ¼-in. depth in the one-dimensional models were then imposed on the top surface of their respective profiles in the three-dimensional model. A graphic summary of the temperature histories imposed on the top surface of the three-dimensional model, as well as their respective locations, is shown in Fig. 10.

The ADINAT finite element computer code has explicit as well as implicit integration capabilities in its solution of the governing heat-transfer equations used in the code. The implicit Euler backward method was chosen. This was done to ensure that the nodal spacing and material properties (specific heat and conductivity) interaction would not cause any instabilities, as might have been the case if an explicit (Euler forward method) integration scheme had been selected.

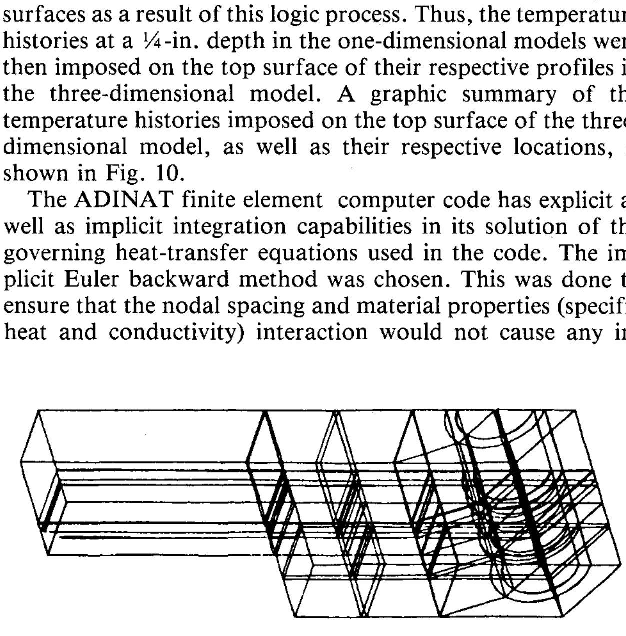

Fig. 9 Insert finite element model.

Temperature Predictions

Typical three-dimensional temperature profiles obtained from the model are shown in Figs. 11 and 12. Shown in the figures are one-dimensional profiles taken at the same location and at the same time in the flight. (See Fig. 6 for a map showing the location of the comparisons.)

An area of principal interest in the outcome of the three-dimensional analysis was in the vicinity of the slip-cast fused silica (SCFS) window, where the cooling effect of three-dimensional heat flow in the structure served to reduce substantially the window and RF probe temperatures in depth. Figure 13 depicts the three-dimensional temperature field in

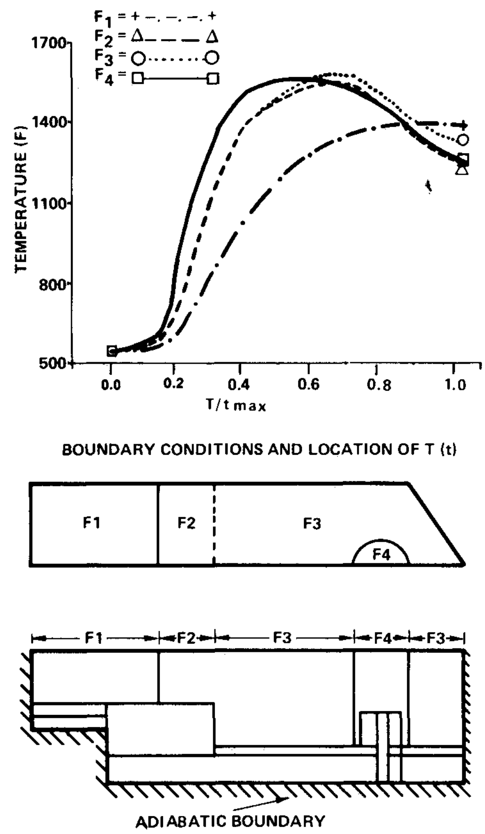

Fig. 10 Three-dimensional model boundary conditions—temperature histories, *T(t)*.

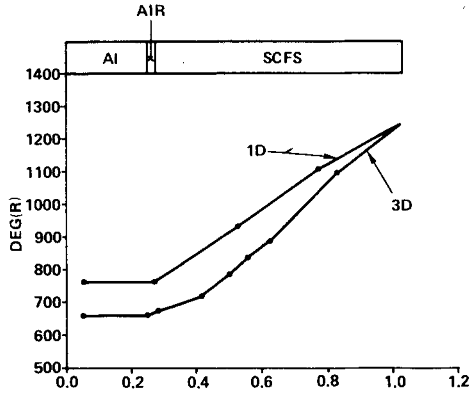

Fig. 11 Comparison of one-dimensional and three-dimensional temperature profiles in slip-cast fused silica at time = max.

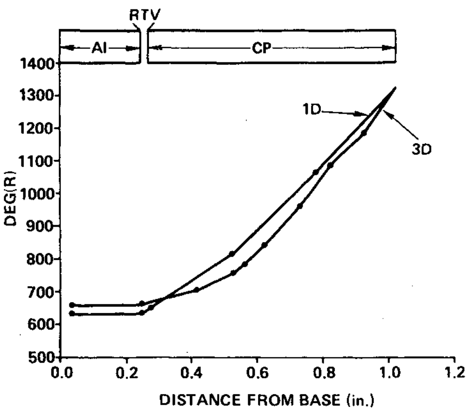

Fig. 12 Comparison of one-dimensional and three-dimensional temperature profiles in carbon phenolic at time = max.

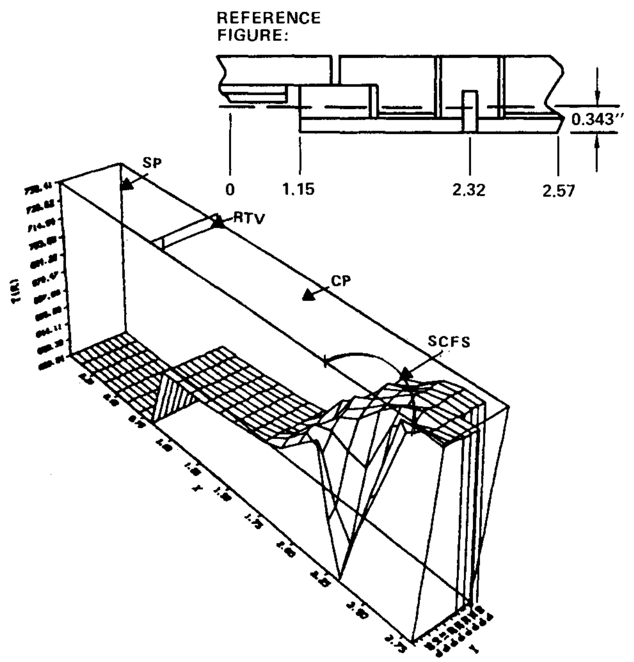

Fig. 13 Temperature plot at 0.343 in. from base of aluminum at $T = T$max.

the model, demonstrating graphically the structural cooling impact of the base structure on the graphite phenolic as well as the thermal isolation in the probe due to its surrounding air gap and low conductivity of the material.

Future Plans

The approach taken—that of sequencing multiple computational routines to develop temperatures in a multidimensional field—has indicated potential as a viable, cost-effective analytical tool. As the current program and following program proceed, the technique will be developed further by introduction of input/output routines and a welcome infusion of test data.

In the current program a number of the thermocouples will be installed on ground-and flight-test vehicles by Sandia National Laboratories, and comparisons will be made between predictions and flight measurements.

Appendix

Here follow brief descriptions of the computer codes used in the analysis:

ADINAT (Automatic Dynamic Incremental Nonlinear Analysis of Temperature): A computer program for the analysis of linear, nonlinear, steadystate, and transient heat conduction of one-, two-, and three-dimensional domains. The program can handle time-dependent flux, convection, and radiation boundary conditions and temperature-dependent material properties including phase change. ADINAT was developed at MIT and represents state-of-the-art in computer systems implementation, numerical analysis, and finite element heat conduction analysis.

CMA: "The Charring Material Ablation program is an implicit, finite-difference computational procedure for computing the one-dimensional transient response of a material which can ablate at one boundary and which can decompose in depth. The program permits up to 20 different materials, of which the first two are reserved for the ablator....The ablating-surface boundary condition may be convection-radiation heating with coupled mass transfer, including the effects of unequal heat and mass transfer coefficients (nonunity Lewis number) and unequal mass diffusion coefficients. Surface thermochemistry computations presume thermochemical equilibrium at the surface....Geometric configurations which may be considered are one-dimensional flat plate, spherical, cylindrical (internal or external ablation), arbitrary cross-section as a function of depth....The inputs include material characteristics of the ablator....Outputs include mass loss rates, surface recession rates, and temperature profiles."[4] The codes have been modified by Sandia National Laboratories to provide expanded capabilities in both calculations and plotting.

GIFTS (Graphics-oriented Interactive Finite Element Time-sharing Systems): A graphics-oriented collection of modules that build and operate on a standardized data base. The modules are designed to fit a relatively small core area; therefore, they are specifically suited to operate in an interactive time-sharing mode. The system may be used as a stand-alone linear finite element analysis package for beam and plate structure evaluation or as a pre- and postprocessor for other programs.

SAAS-III: "The finite element method is used to determine the displacements, stresses, and strains in axisymmetric and plane solids with different orthotropic, temperature-dependent material properties in tension and compression, including the effects of internal pore fluid pressures and thermal stresses. The mechanical loads can be surface pressures, surface shears, and nodal point forces as well as acceleration or angular velocity. The continuous solid is replaced by a system of elements with triangular or quadrilateral cross-sections. Accordingly, the method is valid for solids that are composed of many different materials and which have complex geometry. Two-dimensional mesh generation and temperature interpolation features allow the computer program to be readily used. The convergence of the method to exact answers with diminishing element size is demonstrated and discussed."[3]

Acknowledgments

This work was performed under BIM-SWERVE Letter Contract 52-1756 with Sandia National Laboratories. The technical approach presented in this paper could not have been implemented without the valuable contributions of aerodynamic heating calculations, ablation code, material properties, and test data received from S. Beard, S. McAlees, R. Sheldahl, W. Williamson, and G. Wright of Sandia National Laboratories, as well as technical support from M. Kizner and S. Caruso of Raytheon.

References

[1] "A Finite Element Program for Automatic Dynamic Incremental Nonlinear Analysis of Temperatures," ADINA Engineering Inc., Watertown, MA, AE 81-2, Sept. 1981.

[2]Hussein, A.K. and McCabe, M.W., "Graphics-Oriented Interactive Finite Element Time Sharing System," University of Arizona, Tucson, April 17, 1981.

[3]Crose, J.G. and Jones, R.M., "Finite Element Analysis of Axisymmetric and Plane Solids with Different Orthotropic Temperature Dependent (SAAS-III) Material Properties in Tension and Compression, The Aerospace Corporation, San Bernardino, CA, Rept. Aerospace TR-0059 (S6816-53)-1, June 1971.

[4]Lauger, L.M., Kaestner, P.C., and Blackwell, B.F., " Operation Instructions for Charring Material Ablation Code," Sandia National Laboratories, Albuquerque, NM, SLA-73-0745, Aug. 1973.

[5]Moyer, C.B. and Rindel, R.A., " Finite Difference Solution for the In-Depth Response of Charring Materials Considering Surface Chemical and Energy Balances," Aerotherm Corporation, Mountain View, CA, Final Rept. 66-7, March 1967; also NASA CR-1061, June 1968.

[6]Rindel, R.A., Clark, K.J., and Moyer, C.B., "Experimental and Theoretical Analysis of Ablative Material Response in a Liquid-Propellant Rocket Engine," *4th Quarterly Progress Report, July 1-Sept. 30, 1966*, Mountain View, CA, Aerotherm Project No. 7003, Vidya Project No. 9279, Table 1, p. 23; also NASA CR-72301, Sept. 1967.

[7]Gibbs, N.E., Poole, W.G. Jr., and Stockmeyer, P.K., "An Algorithm for Reducing the Bandwidth and Profile of a Sparse Matrix," *SIAM Journal of Numerical Analysis,* Vol. 13, 1976, pp. 236-250.